Cell and Tissue Research (2021) 385:713–726
https://doi.org/10.1007/s00441-021-03460-5

REGULAR ARTICLE

CD9-positive cells in the intermediate lobe of the pituitary gland are important supplier for prolactin-producing cells in the anterior lobe

Kotaro Horiguchi[1] · Ken Fujiwara[2] · Yoshito Takeda[3] · Takashi Nakakura[4] · Takehiro Tsukada[5] · Saishu Yoshida[6] · Rumi Hasegawa[1] · Shu Takigami[1] · Shunji Ohsako[1]

Received: 10 November 2020 / Accepted: 8 April 2021 / Published online: 7 May 2021

Abstract

A supply of hormone-producing cells from stem/progenitor cells is critical to sustain the endocrine activity of the pituitary gland. In the adenohypophysis composing the anterior and intermediate lobe (AL and IL, respectively), stem/progenitor cells expressing sex-determining region Y-box 2 (SOX2) and S100β are located in the marginal cell layer (MCL) facing Rathke's cleft (primary niche) and the parenchyma of the AL (secondary niche). Our previous studies using mice and rats indicated that the tetraspanin superfamily CD9 and CD81 are expressed in S100β/SOX2-positive cells of primary and secondary niches (named CD9/CD81/S100β/SOX2-positive cell), and the cells located in the AL-side niches exhibit plasticity and multipotency. However, it is unclear whether CD9/CD81/S100β/SOX2-positive cells in the IL-side primary niche are stem/progenitor cells for the AL or IL. Here, we successfully isolated pure CD9/CD81/S100β/SOX2-positive cells from the IL-side primary niche. They had a higher level of S100β and SOX2 mRNA and a greater pituisphere forming capacity than those of CD9/CD81/S100β/SOX2-positive cells isolated from the AL. They also had capacity to differentiate into all types of adenohypophyseal hormone-producing cells, concomitantly with the loss of CD9 expression. Loss of CD9 and CD81 function in CD9/CD81/S100β/SOX2-positive cells by siRNA treatment impaired prolactin cell differentiation. Consistently, in the pituitary gland of CD9/CD81 double knockout mice, dysgenesis of the MCL and a lower population of prolactin cells were observed. These results suggest that the CD9/CD81/S100β/SOX2-positive cells in the MCL of the IL-side are potential suppliers of adult core stem cells in the AL.

Keywords CD9 · Pituitary · Prolactin · SOX2 · The intermediate lobe

✉ Kotaro Horiguchi
kota@ks.kyorin-u.ac.jp

[1] Laboratory of Anatomy and Cell Biology, Department of Health Sciences, Kyorin University, 5-4-1 Shimorenjaku, Mitaka, Tokyo 181-8612, Japan

[2] Department of Biological Science, Faculty of Science, Kanagawa University, 2946 Tsuchiya, Hiratsuka, Kanagawa 259-1293, Japan

[3] Department of Respiratory Medicine and Clinical Immunology, Osaka University Graduate School of Medicine, 2-2 Yamadaoka, Suita 565-0871, Japan

[4] Department of Anatomy, Graduate School of Medicine, Teikyo University, 2-11-1 Kaga, Itabashi, Tokyo 173-8605, Japan

[5] Department of Biomolecular Science, Faculty of Science, Toho University, 2-2-1 Miyama, Funabashi, Chiba 274-8510, Japan

[6] Department of Biochemistry, The Jikei University School of Medicine, 3-25-8 Nishi-shinbashi, Minato-ku, Tokyo 105-8461, Japan

Introduction

The pituitary gland has important roles in maintaining homeostasis through hormone production. The mammalian pituitary gland is composed of two anatomically different entities: the adenohypophysis is composed of the anterior and intermediate lobes (AL and IL, respectively; note that the primate IL is rudimentary), and the neurohypophysis of the posterior lobe (PL). The AL contains five types of hormone-producing cells, together with non-hormonal cells such as S100β-positive cells and fenestrated sinusoids (i.e., endothelial cells and pericytes). The S100β-positive cells in the AL are known to comprise heterogeneous populations including folliculo-stellate cells that play multiple biological roles. However, recent studies indicate that the majority of S100β-positive cells are predicted as stem/progenitor cells because they express the stem cell marker, sex-determining region Y-box 2 (SOX2) (Fauquier et al. 2008; Vankelecom

and Chen 2014; Yoshida et al. 2016b; Horiguchi et al. 2018, 2020a).

A continuous supply of mature cells from stem/progenitor cells is important for sustained cell turnover in the AL. Pituitary stem/progenitor cells sustain their stemness properties in niches where growth factors, cell surface proteins, and extracellular matrices are available. In the adult adenohypophysis, SOX2-positive cells located along the AL-side and IL-side marginal cell layer (MCL) facing Rathke's cleft, and the SOX2-positive cell clusters scattered throughout the parenchyma are proposed to act as the primary and secondary stem/progenitor cell niches, respectively (Chen et al. 2005; Gremeaux et al. 2012; Vankelecom and Chen 2014; Yoshida et al. 2016a). However, it is unclear whether there are differences in the cellular properties between SOX2-positive cells in the MCL and parenchymal niches, as their isolation method has not been established. Our previous study demonstrated the isolation of SOX2-positive cell clusters in the parenchymal niche by taking advantage of its tight structure that is resistant to protease treatment, and confirmed their differentiation capacity into hormone-producing cells by in vitro differentiation (Yoshida et al. 2016b). We also found that the tetraspanin superfamily CD9 and CD81 are novel specific markers for a subpopulation of SOX2-positive cells in the MCL and parenchymal niches of the rodent pituitary, but not for SOX2-positive cells in the PL (Horiguchi et al. 2018). Very recently, we successfully isolated SOX2-positive cells from the AL-side MCL and parenchymal niches using anti-CD9 antibody treatment together with the pluriBead-cascade cell isolation system, and found that a subset of the isolated CD9-, CD81, S100β-, and SOX2-quadruple positive (CD9/CD81/S100β/SOX2-positive) cells has potential to differentiate into endothelial cells and hormone-producing cells of the AL (Horiguchi et al. 2018). Around the same time, Jin et al. (Jin et al. 2018) generated CD9 and CD81 double-knockout (CD9/CD81 DKO) mice. The DKO mice at 6 months old had an elevated aging score compared to wild-type mice, although they grew normal until 3 weeks. At 80 weeks old, both male and female CD9/CD81 DKO mice progressively lost their body weight without significant decrease in food consumption. CD9/CD81 DKO mice also showed other accelerated aging phenotypes including kyphosis, decreased bone mineral density, and reduced volume of muscle and visceral adipose tissues. Interestingly, it is of note that CD9/CD81 DKO mice exhibited infertility with atrophy in the pituitary gland. These findings suggest that CD9 and CD81 play an important role in the differentiation and proliferation of CD9/CD81/S100β/SOX2-positive stem/progenitor cells in the adult AL.

The present study aimed to isolate CD9/CD81/S100β/SOX2-positive cells from the IL-side MCL-niche to compare the cellular properties (proliferation activity, pituisphere forming capacity, and differentiation potential into hormone-producing cells of the AL) of CD9/CD81/S100β/SOX2-positive cells in the AL. We also examined the roles of CD9 and CD81 in the CD9/CD81/S100β/SOX2-positive cells. Finally, based on the in vitro results obtained using isolated IL-side CD9/CD81/S100β/SOX2-positive cells, we performed a detailed histological analysis of the pituitary from CD9/CD81 DKO mice.

Materials and methods

Animals

Male Wistar rats were purchased from Japan SLC, Inc. (Shizuoka, Japan). The day of birth was designated as postnatal day 0 (P0). Eight- to 10-week-old rats weighing 200–250 g were provided ad libitum access to food and water and were housed under a 12-h light/dark cycle. Rats were sacrificed by exsanguination from the right atrium under deep anaesthesia (0.15 mg/kg of medetomidine, Zenyaku Kogyo, Tokyo, Japan, 2.0 mg/kg of midazolam, SANDOZ, Tokyo, Japan, and 2.5 mg/kg of butorphanol, Meiji Seika Pharma, Tokyo, Japan). Then, Hanks' balanced salt solution (Thermo Fisher Scientific, Waltham, MA, USA) and 4% paraformaldehyde in 0.05 M phosphate buffer (PB; pH 7.4) were perfused from the aorta for cell culture and for histological analyses, respectively. Pituitary tissues fixed with 10% formalin and the serum from CD9/CD81 DKO mice were gifts from Dr. Takeda of Osaka University. These mice were backcrossed to the C57BL/6 J background. The present study was approved by the Committee on Animal Experiments of Kyorin University based on the NIH Guidelines for the Care and Use of Laboratory Animals.

Tissue preparation

Cryosections. Tissue preparation for cryosections was performed as described previously (Horiguchi et al. 2014). Frozen frontal sections of the rat pituitary (8 µm thickness) were obtained using a cryostat (Tissue-Tek Polar DM; Sakura Finetek, Tokyo, Japan).

Paraffin-embedded sections. Fixed pituitary tissues of CD9/CD81 DKO mice were processed routinely and embedded in Pathoprep embedding media (FUJIFILM Wako Pure Chemical Corp., Tokyo, Japan). Sagittal sections. (5 µm) were prepared using an ultramicrotome (Ultracut UCT; Leica).

Immunohistochemistry and immunocytochemistry

Immunohistochemistry and immunocytochemistry were performed as described previously (Horiguchi et al. 2014).

The primary and secondary antibodies used are listed in Supplementary Table 1. The absence of an observable nonspecific reaction was confirmed using normal mouse, rabbit, or goat serum (data not shown). Sections were scanned using an epifluorescence microscope (BX61, Olympus, Tokyo, Japan) with the CellSens Dimension system (Olympus).

In situ hybridisation

In situ hybridisation was performed with digoxigenin-labelled cRNA probes or using a solution from the HNPP Fluorescent Detection Kit (Roche Diagnostics, Basel, Switzerland) as described in our previous report (Horiguchi et al. 2016). The following DNA fragments were amplified from mouse pituitary cDNA by PCR: *mouse Prl* with forward (5′-TGGTTCTCTCAGGCCATCTT-3′) and reverse (5′-ATCCCATTTCCTTTGGCTTC-3′) primers. A control experiment using the sense cRNA probe was performed, and no specific signal was detected (data not shown). Cells were scanned using a microscope (BX61, Olympus).

qPCR

qPCR was performed as described previously (Horiguchi et al. 2016). Using TRIzol Reagent (Life Technologies), total RNA was extracted from CD9-positive and negative fractions and pituispheres was then treated with RNase-free DNase I (1 U/tube; Promega, Madison, WI, USA) according to the manufacturer's instructions. cDNA was synthesised using the PrimeScript RT reagent kit (Takara, Otsu, Japan) with oligo-$(dT)_{20}$ primers (Life Technologies). Briefly, qPCR assays were conducted on a Thermal Cycler Dice Real Time System II (Takara, Shiga, Japan) using gene-specific primers and SYBR Premix Ex Taq II (Takara) containing SYBR Green I. The gene-specific primer sequences used are listed in Supplementary Table 2. For normalisation, β-actin (*Actb*) levels were quantified. The relative gene expression was calculated by comparing the cycle times for each target PCR. Cycle threshold values were converted to relative gene expression levels using the $2^{-(\Delta Ct\ sample\ -\ \Delta Ct\ control)}$ method.

Isolation of CD9-positive cells

Pituitary glands of male Wistar rats were dissected, and the AL was manually separated from the pituitary gland using tweezers; the AL and IL/PL tissues were enzymatically digested to disperse their cells as described previously (Horiguchi et al. 2008). Dispersed cells were counted using a haemocytometer and CD9-positive cells were specifically isolated using a Universal Mouse pluriBeads kit (pluriSelect, San Diego, CA, USA) along with a monoclonal anti-rat CD9 antibody (BD Biosciences, San Jose, CA, USA) (Horiguchi et al. 2016, 2018). CD9-positive and -negative cells were processed for smear preparation, qPCR, cultivation, and immunocytochemistry. After immunocytochemistry, using a 40-fold objective lens, 10 random fields (157.5 × 210 mm rectangle) containing CD9-positive cells were captured in each well. The populations of CD9-positive cells were counted using the CellSens Dimension system (Olympus). Three individual experiments were carried out for the cell counting.

Small interfering RNA (siRNA) knockdown

CD9-positive cells isolated from IL/PL tissues ("IL-side CD9-positive cells" containing CD9-positive IL-side marginal cells) and from AL tissues ("AL-side CD9-positive cells" containing CD9-positive AL-side marginal and parenchymal cells) were plated at 1.0×10^5 cells/cm^2 on 8-well glass chamber slides. The cells were then cultured for 24 h in 500 µL DMEM/F-12 with 0.5% bovine serum albumin (BSA, Sigma Sigma-Aldrich, St. Louis, MO, USA) at 37 °C in a humidified atmosphere with 5% CO_2 and 95% air. For small interfering RNA (siRNA) transfection, the culture medium was replaced with 500 µL of DMEM/F-12 with 0.5% BSA, supplemented with the transfection reagent (INTERFERin at 1:100 v/v; PolyPlus Transfection, Illkirch, France) and siRNAs against *Cd9* mRNA (0.2 µM Mm_*Cd9*_1 and 0.2 µM Mm_*Cd81*_1; Qiagen, Venlo, Netherlands), followed by an additional 24 h incubation. A non-silencing siRNA without homology to any known mammalian gene was used as a negative control (SI03650325; Qiagen). After siRNA treatment, the cells were used for the sphere formation assay.

Proliferation assay

To visualise the proliferative activities of the cells, the nucleotide analogue 5-bromo-2′-deoxyuridine (BrdU, Rockland Inc., Limerick, PA, USA) was added at a concentration of 3 µg/mL to the primary culture of CD9/CD81/S100β/SOX2-positive cells on the laminin coated surface for 24 h, after adding siRNAs against *Cd9* and *Cd81* mRNA (Horiguchi et al. 2020b). Cells were fixed with 4% paraformaldehyde in 0.025 M PB (pH 7.4) for 15 min at 20–23 °C and were then treated with 4 N HCl in PBS for 10 min. Immunocytochemistry for BrdU was performed as described above. Ten fields per well were randomly captured using the CellSens Dimension system (Olympus) installed on a microscope (BX61, Olympus) with a 40-fold objective lens.

Growth of pituispheres

IL- and AL-side CD9-positive cells were plated on 35-mm non-treated dishes (AGC Techno Glass, Shizuoka, Japan)

at a density of 25,000 cells/dish in DMEM/F-12 containing B27 supplement (1:50; Thermo Fisher Scientific), N2 supplement (1:100; FUJIFILM Wako Pure Chemical Corp.), BSA (0.5%; Sigma), bFGF (20 ng/ml), and EGF (20 ng/ml). The cells were incubated in humidified chambers with 5% CO_2 at 37 °C. Pituisphere growth was assessed 5 days after plating. Pituispheres were then collected manually by pipetting under a microscope. Differentiation induction of pituispheres into GH- and PRL-producing cell lineages was conducted using an induction procedure according to Suga et al. (2011) with some modifications. Briefly, the pituispheres were cultured by the overlay 3D culture method on Matrigel-coated 16-well chamber slides (0.4 cm^2/well) (Thermo Fisher Scientific) with 20 ng/ml each of bFGF and EGF, and 20% KnockOut Serum Replacement (KSR) (Thermo Fisher Scientific) for 4 days, followed by replacement with medium including 6-bromoindirubin-3′-oxime (BIO) (GSK3β-inhibitor, 250 nM; FUJIFILM Wako Pure Chemical Corp.) and cultivation for another 10 days. After immunocytochemistry, the population of immunopositive cells were manually counted by observing a sphere along z axis using a 60-fold objective lens. More than 10 random spheres/experiment were counted and three individual experiments were carried out.

Measurement of PRL, GH, and IGF-I

Serum PRL, GH, and IGF-I concentrations in CD9/CD81 DKO mice were measured using commercially available ELISA kits (PRL, Abcam, Cambridge, UK; GH, Merk Millipore, Darmstadt, Germany; IGF-I, Proteintec, Rosemont, IL, USA) according to the manufacturer's instructions. The blood samples were collected between 0900 and 1000 h from each three male mice at 75–85 weeks old.

Statistical analysis

Data are presented as the mean ± SEM of at least three preparations for each group. Student's *t* test after *F* tests was used for two-group comparison, and Dunnett's test was for multiple comparisons. *P* values less than 0.05 were considered statistically significant.

Results

Localisation of CD9/CD81/S100β/SOX2-positive cells in the adult rat pituitary gland

To determine the structure of the MCL, we stained the pituitary gland with haematoxylin and eosin (HE). Figure 1a–d show a frontal view of the pituitary gland from an adult male Wistar rat (P60). The MCL faces Rathke's cleft, and the AL-side and IL-side are connected at the wedge zone (Fig. 1a–d). There are also several bridges across the Rathke's cleft between the AL-side and IL-side (Fig. 1d). As indicated by CD9 immunohistochemistry (Fig. 1e, f) and double immunohistochemistry (Fig. 1g–i), CD9-positive cells were located at the MCL of the AL and IL, and in the parenchyma of the AL, but not in the PL; further, they expressed CD81, SOX2, and S100β.

Purification and characterisation of IL-side CD9/CD81/S100β/SOX2-positive cells

We next attempted to purify CD9/CD81/S100β/SOX2-positive cells from the MCL of the IL using a monoclonal anti-rat CD9 antibody combined with the pluriBead-cascade cell isolation system. Isolated CD9-positive and -negative cell fractions were processed for smear preparation, and then used for double immunocytochemistry for CD9 and proopiomelanocortin (POMC: IL hormone). We observed that most of the cells in the CD9-positive cell fraction were immunopositive for CD9 (Fig. 2a–c), whereas the cells in CD9-negative fraction were immunopositive for POMC, but not for CD9 (Fig. 2d–f). The proportion of CD9-positive cells in the CD9-positive fraction was 92.2 ± 1.2% (data not shown). The *Cd9* mRNA level was 3.0-fold higher in the CD9-positive cell fraction than in the CD9-negative cell fraction (Fig. 2g). Conversely, the mRNA level of *Pomc* was significantly lower in the CD9-positive cell fraction than that in the CD9-negative fraction (Fig. 2g). Consistent with the immunohistochemistry results in Fig. 1g–i, *Cd81*, *S100β*, and *Sox2* were expressed at higher levels in the CD9-positive cell fraction (Fig. 2g). Figure 2h shows the comparison of gene expression between the IL-side and AL-side CD9-positive cells. *Cd9*, *Cd81*, and *Sox2,* but not *S100β* expression, was significantly higher in the IL-side CD9-positive cells.

Effect of Cd9 and Cd81 siRNAs on IL-side CD9/CD81/S100β/SOX2-positive cells

CD9 has the ability to associate with various integrins (Boucheix and Rubinstein 2001; Hemler 2005). Recently, we revealed that CD9 sustains the proliferation activity of AL-side CD9-positive cells through integrin signalling (Horiguchi et al. 2018). The present study examined the functional roles of CD9 and CD81 in IL-side CD9-positive cells. To this end, we knocked down *Cd9* and/or *Cd81* gene expression in IL-side CD9-positive cells using siRNAs. *Cd9* and/or *Cd81* expression levels were successfully downregulated by the *Cd9* and/or *Cd81* siRNAs (Fig. 3a). The expression of *S100β* was also downregulated by *Cd9* and/or *Cd81* siRNAs, whereas *Sox2* expression was unchanged (Fig. 3a). Proliferation activity assessed by BrdU immunocytochemistry showed that *Cd9* and *Cd81* siRNAs clearly decreased the

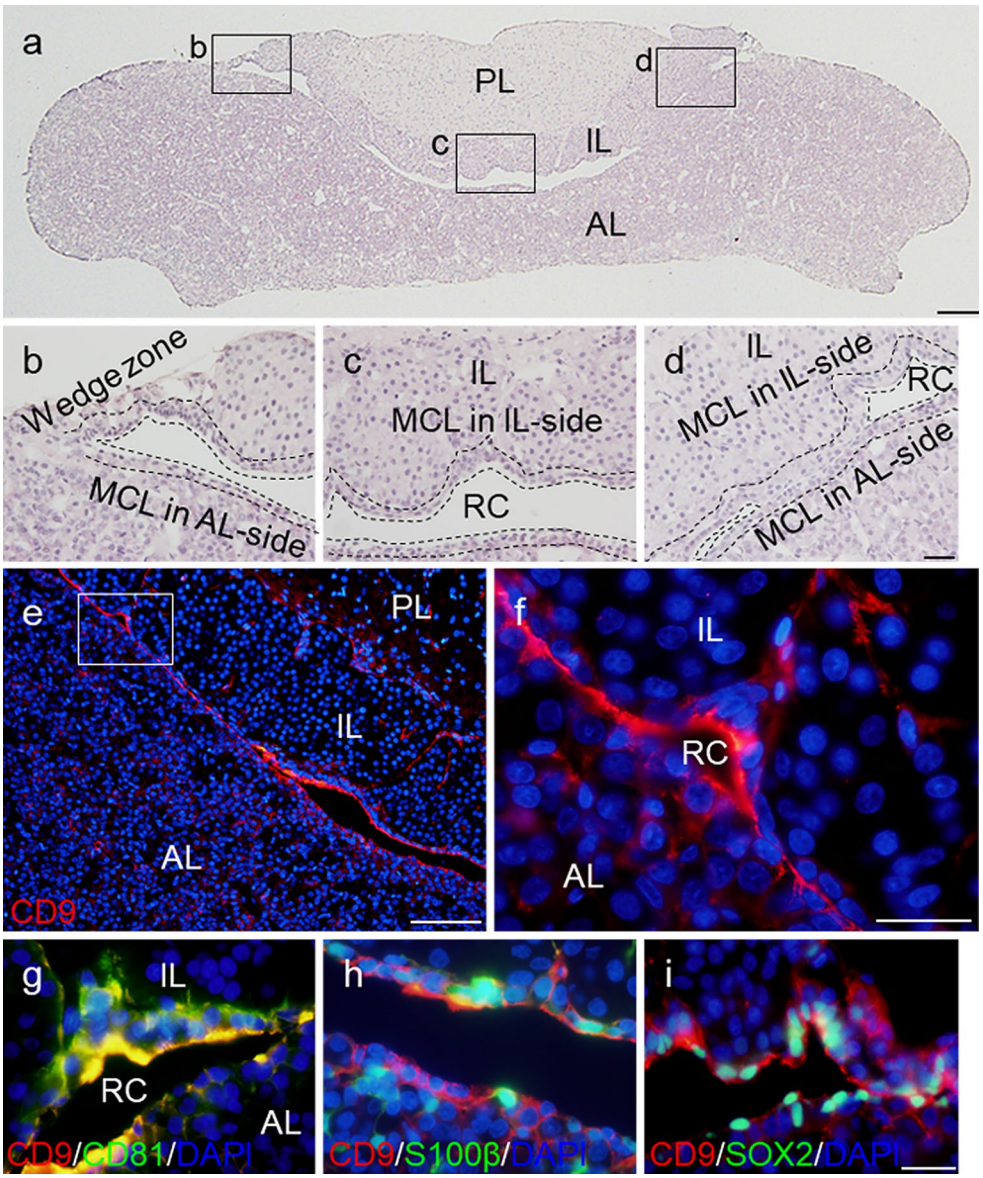

Fig. 1 Expression of CD9 in the MCL of the IL- and AL-sides. **a**–**i** Pituitary gland of male Wistar rat P60. **a**–**d** HE staining. High magnification of the boxed area in upper panels is shown in the lower panels. **e** and **f** Immunohistochemistry for CD9 (red). Nuclear staining with DAPI is shown in blue. **g**–**i** Double immunohistochemistry for CD9 (red) and CD81 **g**, or S100β **h**, or SOX2 **i** (green). Scale bars, 200 μm **a**, 100 μm **e**, 50 μm **d**, **f**, and **i**. AL anterior lobe, IL intermediate lobe, PL posterior lobe, RC Rathke's cleft, MCL marginal cell layer

proliferation activity in IL-side CD9-positive cells compared with the non-silencing siRNA (Fig. 3b, b'). The proportion of BrdU-positive cells among *Cd9* and *Cd81* ($5.7 \pm 0.8\%$) siRNA-treated cells was significantly lower ($P < 0.01$) than that among control cells ($10.9 \pm 1.1\%$) (Fig. 3c); however, the effect of *Cd9* and *Cd81* siRNAs on the proliferation activity was not significantly different between the IL-side and AL-side CD9-positive cells (Fig. 3c).

Pituisphere formation and differentiation capacity of IL-side CD9/CD81/S100β/SOX2-positive cells

To compare the stem/progenitor potential between IL-side and AL-side CD9-positive cells, nonadherent pituispheres were grown in culture and differentiation was induced. Figure 4a and a' show a pituisphere formed using IL-side and AL-side CD9-positive cells after 5-day cultivation.

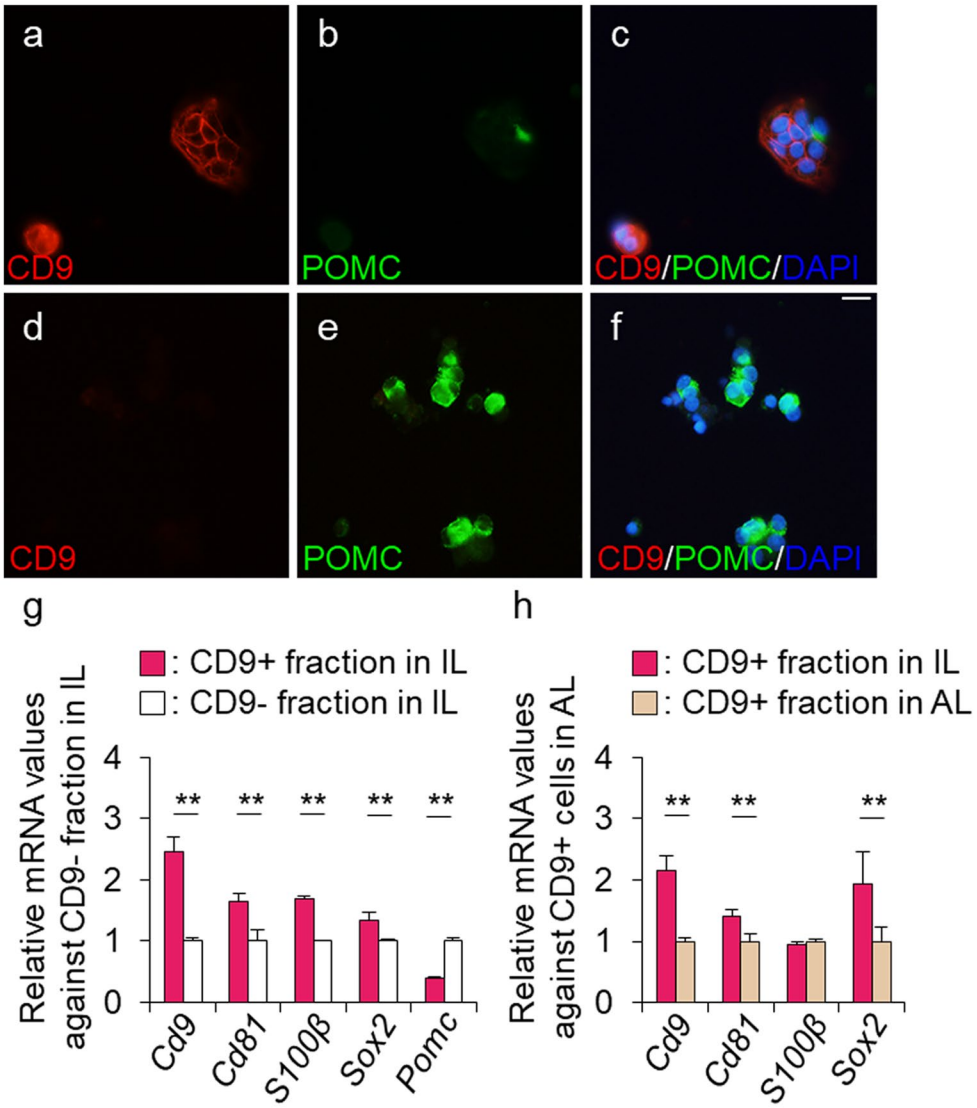

Fig. 2 Isolation of CD9-positive cells from the IL-side MCL. **a**–**f** Double immunofluorescence staining for CD9 and POMC in smear preparations using IL-side CD9-positive cells and -negative fractions. Table shows the proportion of CD9-positive cells among CD9-positive cell fraction. Scale bar, 10 µm. **g** mRNA levels of the indicated genes in IL-side CD9-positive and CD9-negative cell fractions were determined by qPCR (mean ± SEM, $n = 6$), followed by normalisation with an internal control (*Actb*): *Cd9*, *Cd81*, *S100β*, *Sox2*, and *Pomc*. $^{**}P < 0.01$. **h** mRNA levels of the indicated genes in IL-side and AL-side CD9-positive cell fractions were determined by qPCR (mean ± SEM, n = 6), followed by normalisation with an internal control (*Actb*): *Cd9*, *Cd81*, *S100β*, and *Sox2*. $^{**}P < 0.01$

Pituispheres of either IL-side or AL-side CD9-positive cells were similarly stained with CD9 and SOX2 antibodies and could be propagated for more than 2 passages (Fig. 4b–b’’’, IL-side pituisphere; for AL-side pituisphere, see Supplementary Fig. 1a). Pituisphere formation capacity evaluated by the number of pituispheres was significantly higher in IL-side pituispheres (18.0 ± 0.3/well) than that in AL-side pituispheres (10.7 ± 0.4/well, Fig. 4c). To compare the differentiation capacity between IL-side and AL-side pituispheres, immunocytochemistry for AL hormones was performed after 14-day cultivation in differentiation media. Intriguingly, hormone-producing cells were observed in IL-side pituispheres, and these cells were negative for CD9 (Fig. 4d–d”, IL-side pituisphere). The population of hormone-producing cells per total cells in an IL-side pituisphere was 24.2 ± 2.7%, which was comparable to the proportion in an AL-side pituisphere (Fig. 4e). Furthermore, we detected that all types of hormone-producing cells were observed, and that undifferentiated CD9-positive cells sustained the expression of S100β in the IL-side and AL-side pituispheres (Fig. 4f–g”, IL-side pituisphere; for AL-side pituisphere, see Supplementary Fig. 1b). The majority of hormone-producing cells in both IL-side and AL-side pituispheres were GH and PRL cells (Fig. 4h, Supplementary

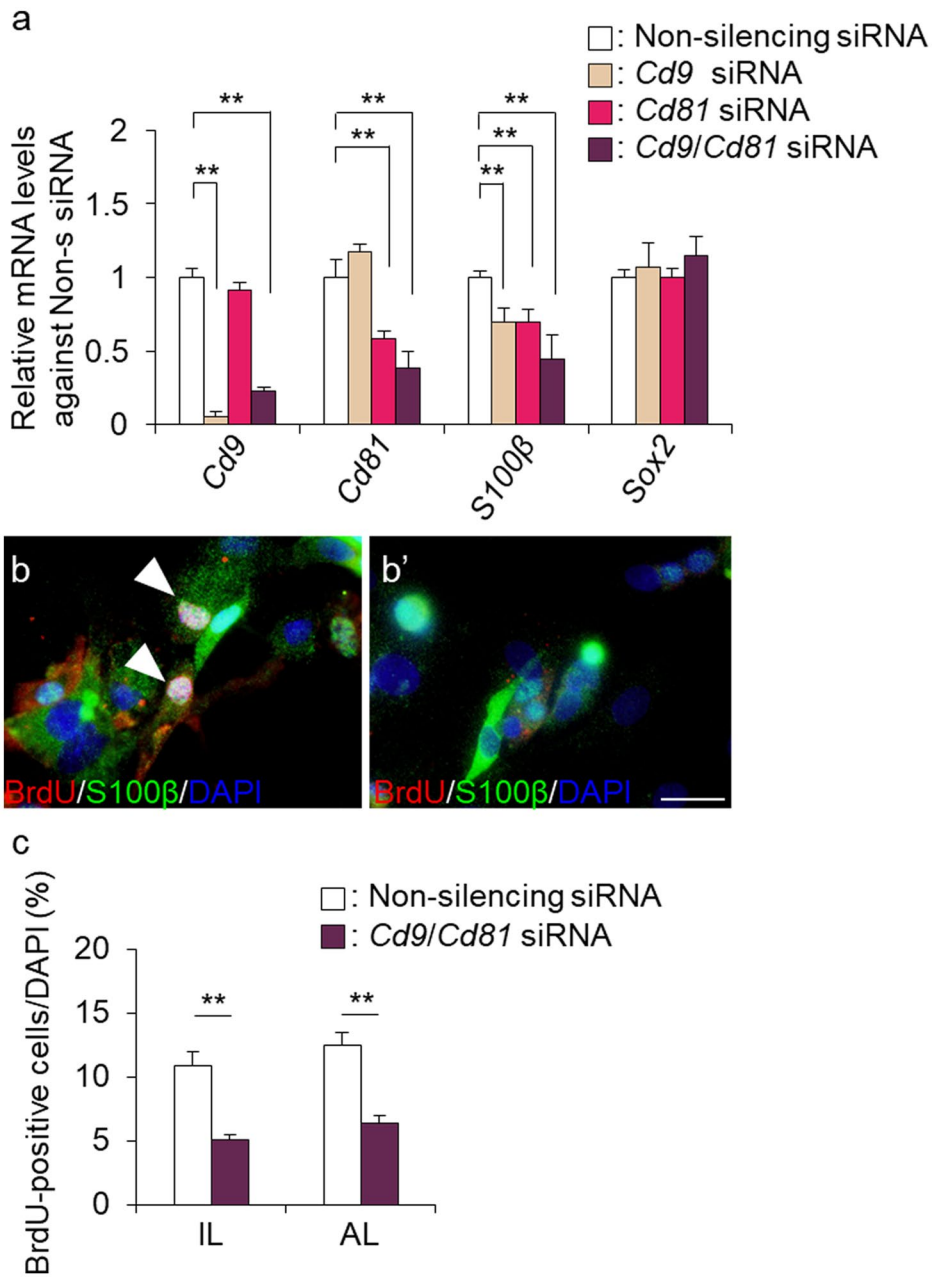

Fig. 3 Downregulation of *Cd9*, *Cd81* mRNA levels by siRNA transfection in IL-side CD9-positive cells. **a** *Cd9*, *Cd81*, *S100β*, and *Sox2* mRNA levels in IL-side CD9-positive cells treated with non-silencing siRNAs or *Cd9*, *Cd81*, or *Cd9/Cd81*-siRNAs for 24 h, as determined by qPCR (mean ± SEM, $n = 6$), followed by normalisation with an internal control (*Actb*). $^{**}P < 0.01$. **b** and **b'** Immunocytochemistry for BrdU (red) and S100β (green) after siRNA transfection for 48 h (**b**, *Non-silencing siRNA*; **b'**, *Cd9/Cd81 siRNA*). $^{**}P < 0.01$. Scale bar, 10 µm. **c** The proportion of BrdU-immunopositive cells among total IL-side or AL-side CD9-positive cells after *Cd9* and *Cd81*-siRNA treatments

Fig. 1c). We then examined the gene expression profile of IL-side and AL-side pituispheres before and after induction. In both pituispheres, *Cd9*, *Cd81*, *S100b*, and *Sox2* mRNA levels were significantly lower before induction, whereas *Pit1*, *Gh*, and *Prl* mRNA levels were significantly higher before induction (Fig. 4i, IL-side pituisphere; for AL-side pituisphere, see Supplementary Fig. 1d).

Effect of Cd9 and Cd81 siRNAs on pituisphere formation and differentiation

To check the involvement of CD9 and CD81 in pituisphere formation and differentiation, we knocked down *Cd9* and *Cd81* in IL-side and AL-side pituispheres using siRNAs. *Cd9* and *Cd81* expression were successfully downregulated by *Cd9/Cd81* siRNAs and the resulting pituispheres were immunonegative for CD9 and CD81 (Fig. 5a–b', IL-side pituisphere; for AL-side pituisphere, see Supplementary Fig. 2a, b). Although pituisphere formation activity was decreased by the process of siRNA treatment (Fig. 5c') compared with that without siRNA treatment (Fig. 5c), downregulation of *Cd9* and *Cd81* expression by the siRNAs did not affect pituisphere formation (Fig. 5c–d, IL-side pituisphere; for AL-side pituisphere, see Supplementary Fig. 2c, d). siRNA-treated pituispheres were further cultivated in differentiation media for 14 days to check their differentiation

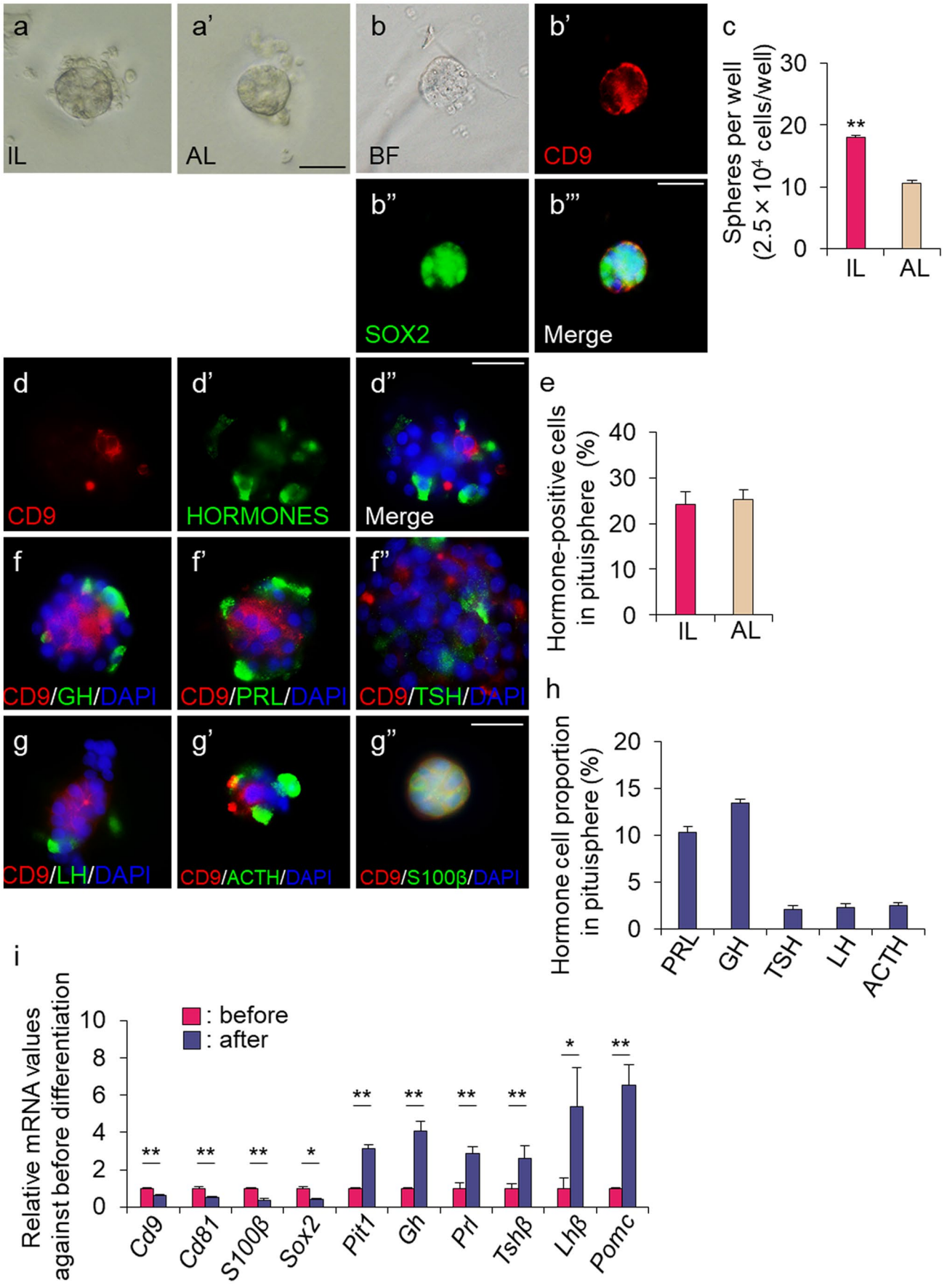
a
IL
a'
AL
b
BF
b'
CD9
b''
SOX2
b'''
Merge
c
Spheres per well
(2.5 × 10^4 cells/well)
30
20
10
0
**
IL
AL
d
CD9
d'
HORMONES
d''
Merge
e
Hormone-positive cells
in pituisphere (%)
40
30
20
10
0
IL
AL
f
CD9/GH/DAPI
f'
CD9/PRL/DAPI
f''
CD9/TSH/DAPI
g
CD9/LH/DAPI
g'
CD9/ACTH/DAPI
g''
CD9/S100β/DAPI
h
Hormone cell proportion
in pituisphere (%)
20
15
10
5
0
PRL
GH
TSH
LH
ACTH
i
Relative mRNA values
against before differentiation
10
8
6
4
2
0
: before
: after
**
**
**
*
**
**
**
**
*
**
Cd9
Cd81
S100β
Sox2
Pit1
Gh
Prl
Tshβ
Lhβ
Pomc

◂**Fig. 4** Pituisphere formation of CD9-positive cells from the IL-side MCL. **a** and **a'** Bright field images of pituispheres before cultivation in 3-D matrigel (**a**, IL-side CD9-positive cells; **a'**, AL-side CD9-positive cells). **b**–**b'''** Double immunofluorescence staining for CD9 and SOX2 in the 2nd passage of a pituisphere from IL-side CD9-positive cells. **b** Bright field image (BF). **b'** CD9 (red). **b''** SOX2 (green). **b'''** The merged image for DAPI (blue), CD9 (red), and SOX2 (green) staining. **c** The number of pituispheres formed by IL- and AL-side CD9-positive cells. $^{**}P<0.01$. **d**–**d'** Double immunocytochemistry for CD9 (red) and hormone-cocktail antibody (green, PRL, GH, TSHβ, LHβ, and ACTH). **e** The proportion of hormone-positive cells in pituispheres formed by IL- and AL-side CD9-positive cells. **f**–**g''** Double immunofluorescence staining for CD9 (red) and GH **f**, or PRL **f'**, TSH **f''**, LH **g**, ACTH **g'**, and S100β **g''** (green) in a pituisphere from IL-side CD9-positive cells after differentiation induction. **h** The proportion of each hormone-positive cell among pituispheres from IL-side CD9-positive cells. **i** mRNA levels of the indicated genes in pituispheres of IL-side CD9-positive cells before or after differentiation induction, determined by qPCR (mean ± SEM, $n=6$), followed by normalisation with an internal control (*Actb*): *Cd9*, *Cd81*, *S100β*, *Sox2*, *Pit1*, *Gh*, *Prl*, *Tshβ*, *Lhβ*, and *Pomc*. $^{**}P<0.01$. $^{*}P<0.05$. Scale bar, 50 µm

capacity. We confirmed that the effect of siRNAs was sustained after induction of differentiation (Fig. 5e, IL-side pituisphere; for AL-side pituisphere, see Supplementary Fig. 2e). Immunocytochemistry for GH and PRL showed that *Cd9*/*Cd81* siRNA-treated pituispheres have more GH cells and less PRL cells compared to those in non-silencing siRNA-treated pituispheres (Fig. 5f, g, IL-side pituisphere; for AL-side pituisphere, see Supplementary Fig. 2f, g). As shown in Supplementary Fig. 2h, DES-treated AL-side pituisphere showed downregulation of *Sox2*, and upregulation of ER alpha (*Era*) and *Prl*.

Histological observation of the pituitary gland in CD9/CD81 DKO mice

A previous study showed that CD9/CD81 DKO mice displayed atrophy in the pituitary gland (Jin et al. 2018); however, a detailed histological analysis has not been done. Therefore, we evaluated the pituitary gland of CD9/CD81 DKO mice based on the results obtained from our pituisphere experiments. Figure 6a–d''' show the general morphology and HE staining of the wild type (WT) and CD9/CD81 DKO mouse pituitary. The pituitary mass of CD9/CD81 DKO mice was smaller than that in WT mice as reported. In CD9/CD81 DKO mice, the IL-side marginal cells were replaced with connective tissue (Fig. 6d'', d''', arrowheads). The relative area of the IL and AL, but not PL, in CD9/CD81 DKO mice was smaller than that in the WT (Fig. 6e, IL 47.8%, AL 38.4%). Although we detected SOX2 and S100β-positive cells in the IL-side and AL-side MCL by immunohistochemistry (Fig. 7a, a'), the proportions in the MCL were significantly lower in CD9/CD81 DKO mice (Fig. 7b). In addition, the proportion of PRL-immunoreactive cells in the parenchyma of AL at CD9/CD81 DKO mice was significantly lower than that in the WT (Fig. 7c–c'), concomitant with the *Prl* mRNA signals evaluated by in situ hybridisation (Fig. 7c''–c'''), whereas the proportions of GH-, TSHβ-, LHβ-, and ACTH-immunoreactive cells were unchanged (Fig. 7d, Supplementary Fig. 3a, b). The proportion of S100β-positive cells in the AL of CD9/CD81 DKO mice was also significantly lower than that in the WT (Fig. 7d, Supplementary Fig. 3c). Finally, we measured the serum PRL, GH and IGF-I concentrations in WT and CD9/CD81 DKO mice (Fig. 7e–e''). Although a slight decrease in serum PRL concentration was observed in CD9/CD81 DKO mice, there was no significant change. In contrast, the serum GH concentration was significantly higher in CD9/CD81 DKO mice irrespective of a similar proportion of GH-immunoreactive cells between the WT and CD9/CD81 DKO mice. Unlike serum GH levels, serum IGF-I levels were lower in CD9/CD81 DKO mice.

Discussion

In the present study, we first isolated CD9/CD81/S100β/SOX2-positive cells from the IL-side MCL utilizing the CD9 antibody. CD9/CD81/S100β/SOX2-positive cells showed sphere formation capacity and could differentiate into all types of AL hormone-producing cells. *Cd9* and *Cd81* knockdown in these cells inhibited their proliferation activity and PRL cell differentiation. Consistently, histological observation of the pituitary gland from CD9/CD81 DKO mice showed dysgenesis of the IL-side MCL and a decreased number of PRL cells in the AL. These findings suggest that IL-side CD9/CD81/S100β/SOX2-positive cells can supply hormone-producing cells to the AL although they are located on the opposite side of Rathke's cleft.

The MCL is proposed to function as a primary niche, contains stem/progenitor cells in different cell cycle and maturation phases. SOX2-positive stem cells in the AL-side MCL are thought to migrate into the parenchyma stem cell clusters (secondary niches) to form an interdigitated, communicating three-dimensional network. The stem cells then move to the glandular area by EMT for differentiation (Vankelecom and Chen 2014). However, it is unknown whether SOX2-positive stem cells in the MCL of IL-side have properties similar to those in the MCL of AL-side. Isolation of these cells will be an important clue to address this question; however, until recently, no isolation method has been successful, because SOX2-positive stem cells are also expressed in the PL. By utilizing the CD9 expression property in SOX2-positive cells of the adenohypophysis but not the neurohypophysis, the present study is the first report to demonstrate isolation of pure SOX2-positive cells from the IL-side MCL. Compared with the gene expressions of CD9-positive cells in the AL, the IL-side CD9-positive cells showed higher levels of stem/progenitor makers (*Sox2* and *S100b*). Furthermore, the pituisphere formation capacity was higher in IL-side CD9-positive cells. Therefore, IL-side CD9/CD81/S100β/

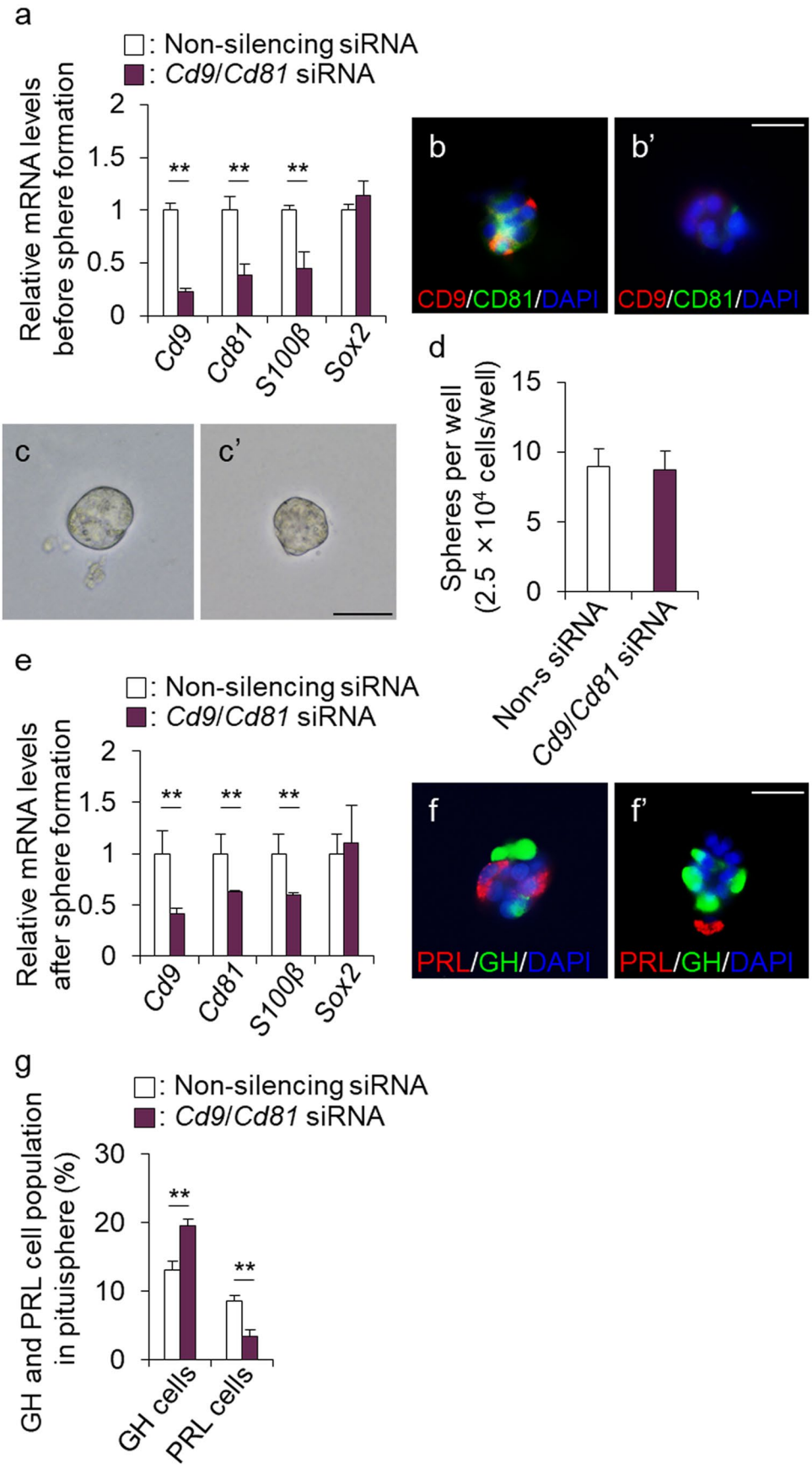

Fig. 5 Differentiation capacity of pituispheres formed using CD9-positive cells of the IL-side in the presence of *Cd9* and *Cd81* siRNA. **a** mRNA levels of the indicated genes in IL-side CD9-positive cells after *Cd9* and *Cd81* siRNA treatment, determined by qPCR (mean ± SEM, $n = 6$), followed by normalisation with an internal control (*Actb*): *Cd9*, *Cd81*, *S100β*, and *Sox2*. $^{**}P < 0.01$. **b** and **b'** Double immunofluorescence staining for CD9 and CD81 in an siRNA-treated pituisphere **b**, non-silencing siRNA; **b'**, *Cd9*/*Cd81* siRNA. **c** and **c'** Bright-field images of pituispheres of CD9-positive cells after siRNA treatment **c**, non-silencing siRNA; **c'**, *Cd9*/*Cd81* siRNA. **d** The number of pituispheres formed by siRNA-treated CD9-positive cells. **e** mRNA levels of the indicated genes in differentiated pituispheres of IL-side CD9-positive cells after *Cd9* and *Cd81* siRNA treatment (white bars, non-silencing siRNA and brown bars, *Cd9*/*Cd81* siRNA) determined by qPCR (mean ± SEM, $n = 6$), followed by normalisation with an internal control (*Actb*): *Cd9*, *Cd81*, *S100β*, and *Sox2*. $^{**}P < 0.01$. **f** and **f'** Double immunofluorescence staining for PRL (red) and GH (green) in siRNA-treated pituispheres **f**, non-silencing siRNA; **f'**, *Cd9*/*Cd81* siRNA. **g** GH and PRL cell population after differentiation of pituispheres from IL-side CD9-positive cells after siRNA treatment. Scale bars, 50 µm

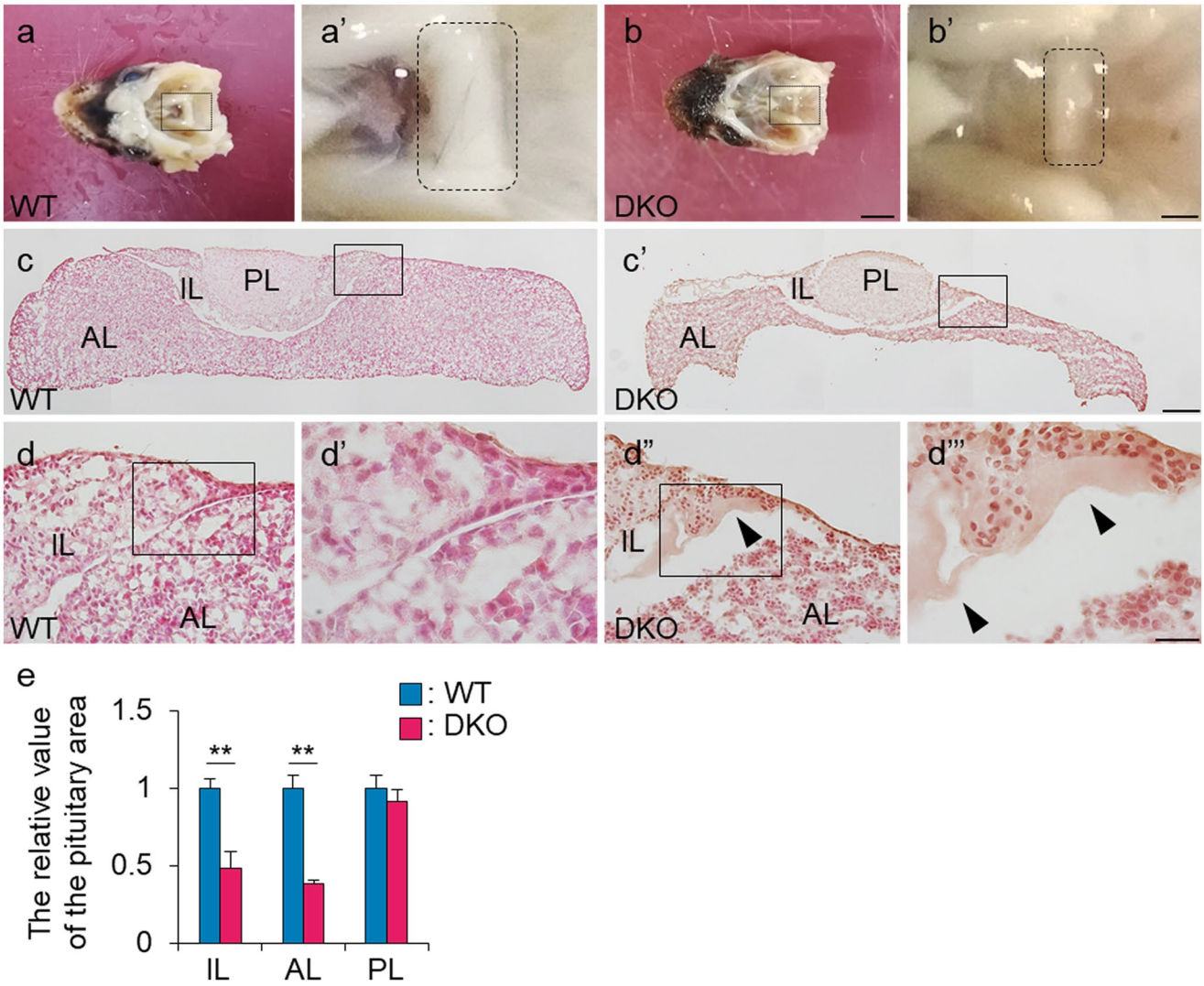

Fig. 6 Histological observation of the pituitary gland in CD9/CD81 DKO mice. **a**–**b'** Images of the pituitary glands of a wild type mouse (WT, **a** and **a'**, 50 weeks old female) and **a** CD9/CD81 DKO mouse (**b** and **b'**, 63 weeks old female). Right panels show a high magnification of the boxed area in the left panels. **c** and **c'** HE staining of the pituitary gland from WT **c** and CD9/CD81 DKO mice **c'**. **d**–**d'''** High magnification of the boxed area in **c**, **c'**, **d**, and **d'**. **e** The size of the anterior, intermediate, and posterior lobe of the pituitary sections, followed by normalisation with those of the WT. AL anterior lobe, IL intermediate lobe, PL posterior lobe, RC Rathke's cleft. Scale bars, 5 mm **b**, 1 mm **b'**, 100 μm **c'**, 20 μm **d'''**

SOX2-positive cells might have higher stemness than that in CD9/CD81/S100β/SOX2-positive cells of the AL.

In the present study, both IL-side and AL-side CD9/CD81/S100β/SOX2-positive cells showed proliferation and pituisphere formation capacities. Knockdown of CD9/CD81 using siRNA resulted in the inhibition of proliferation and PRL cell differentiation in vitro. These findings are in agreement with the phenotype of CD9/CD81 DKO mice. The development of PRL cells appears to be suppressed by glucocorticoids and to be postnatally proceeded by estrogen (Japon et al. 1994; Sato and Watanabe 1998; Matsubara et al. 2001) and IGF-I (Oomizu et al. 1998; Stefaneanu et al. 1999). In fact, mice inactivated for the estrogen receptor (ER) and IGF-I receptor genes exhibit fewer PRL cells (Scully et al. 1997; Ogasawara et al. 2009). As the development of PRL cells is proceeded by estrogen (Matsubara et al. 2001), we cultivated *Cd9*/*Cd81* siRNA-treated pituispheres in the present of DES. DES-treatment downregulated *Sox2* and upregulated ER alpha (*Era*) and *Prl*, indicating the recovery of PRL cell differentiation by DES-treatment. Furthermore, we found that the serum IGF-I level was significantly lower in the CD9/CD81 DKO mice that had a decreased number of PRL cells. These findings suggest that oestrogen and IGF-I may be required for the proliferation and differentiation of PRL cells from CD9/CD81/S100β/SOX2-positive cells. However, it is still

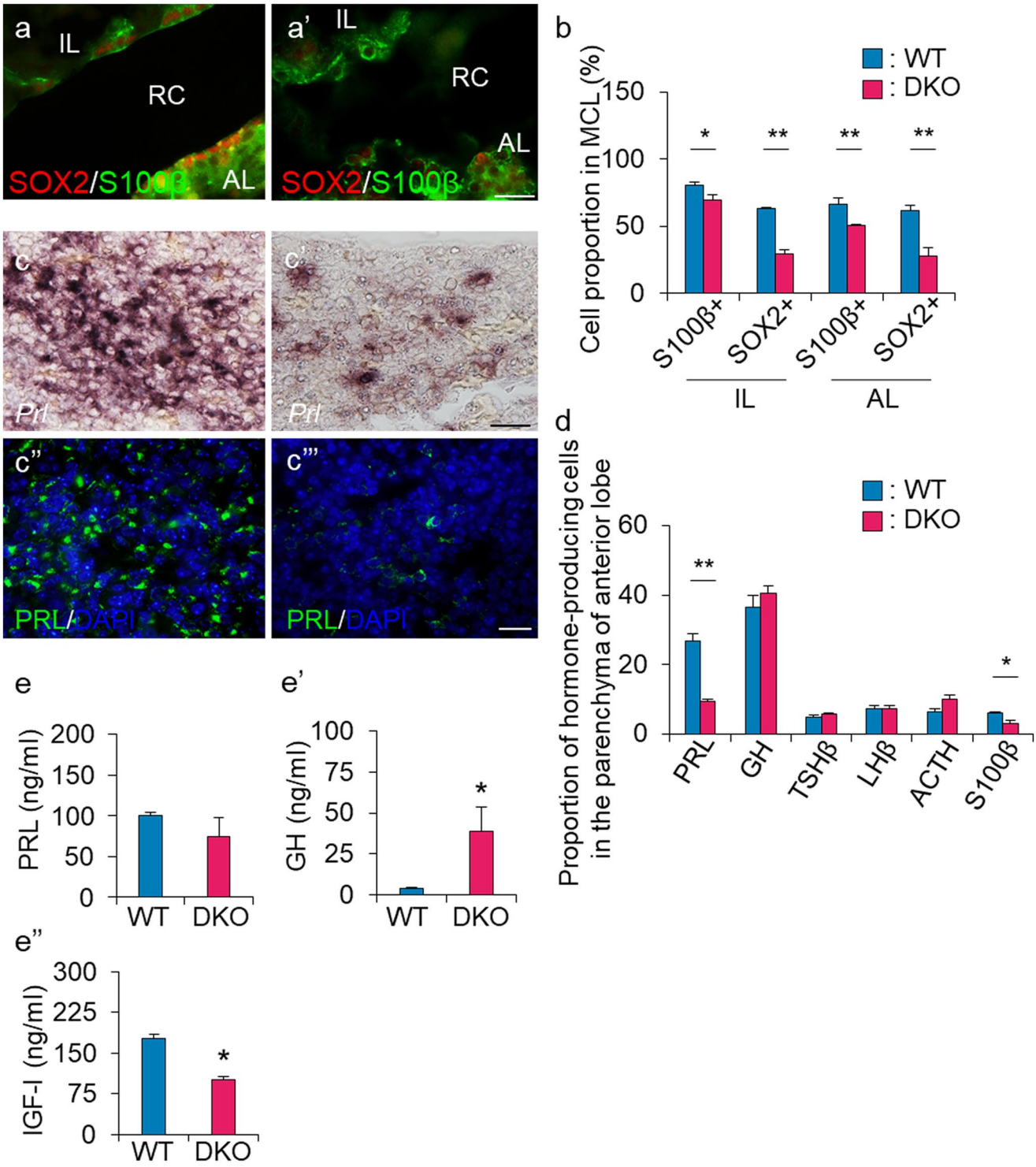

Fig. 7 **a** and **a'** Immunostaining for SOX2 (red) and S100β (green) in the MCL of WT **a** and DKO mice **a'**. **b** The proportion of S100β- and SOX2-positive cells in the IL- and AL-side MCL. **c** and **c'** In situ hybridisation of *Prl* in the parenchyma of AL at WT **c** and CD9/CD81 DKO mice **c'**. **c''** and **c'''** Immunohistochemistry for PRL in the parenchyma of AL at WT **c''** and CD9/CD81 DKO mice **c'''**. **d** The proportion of immunopositive cells for pituitary hormones and for S100β in the parenchyma of the AL in WT and CD9/CD81 DKO mice. **e**-**e''** Serum PRL **e**, GH **e'**, and IGF-I **e''** concentrations in wild-type (WT) and CD9/CD81 DKO mice (DKO) measured by ELISA. AL anterior lobe, IL intermediate lobe, RC Rathke's cleft. Scale bars, 20 μm **a'**, **c'**, **c'''**

unknown why serum GH and IGF-I levels were not correlated in CD9/CD81 DKO mice. Furthermore, the serum PRL and GH levels were not correlated with the proportion of immunoreactive PRL and GH cells in CD9/CD81 DKO mice, respectively. Although further investigation is required, these results imply that CD9 and CD81 influence the secretion of PRL and GH.

CD9/CD81 DKO mice displayed a lower number of PRL cells, but CD9/CD81 DKO did not eliminate all PRL cells from the AL. During early embryonic development of the pituitary gland, CD9-negative SOX2-positive cells first appear in the pituitary primordium and settle in the primary niche. On the contrary, as CD9/CD81/S100β/SOX2-positive cells are first observed in the MCL after birth, it is thought that there are at least two origins of SOX2 stem progenitor cells in the MCL, defined by the presence/absence of CD9 expression. Therefore, the PRL cells in DKO mice may be attributable to CD9-negative SOX2-positive cells, and the most of PRL-producing cells in the WT pituitary may be derived from CD9/CD81/S100β/SOX2-positive stem/progenitor cells in the IL-side MCL. Similar discrepancy was observed in GH cell differentiation in vitro and in vivo; the *Cd9*/*Cd81* siRNA treatment significantly increased GH cell differentiation, whereas the proportions of GH-immunoreactive cells was unaffected in CD9/CD81 DKO mice. One possible explanation is that CD9-negative SOX2-positive cells control total GH population together with CD9/CD81/S100β/SOX2-positive stem/progenitor cells in the IL-side MCL in vivo. However, it should be noted that accelerated aging phenotypes in the CD9/CD81 DKO mice (Jin et al. 2018) might interact with the observed data in the present study, such as increased apoptosis rather than decreased proliferation and differentiation.

In summary, the present study showed that IL-side CD9/CD81/S100β/SOX2-positive cells showed a stemness and differentiation capacity similar to AL-side CD9/CD81/S100β/SOX2-positive cells. Therefore, it is highly possible that they act as pituitary stem/progenitor cells in the primary niche of the adult pituitary and supply progenitor cells to the AL parenchyma (secondary niche). Although it is still unclear how the IL-side CD9/CD81/S100β/SOX2-positive cells migrate to the AL parenchyma, they may migrate through the wedge zone and bridge between the AL-side and IL-side, across Rathke's cleft, as observed in the present study. Further functional analysis using IL-side CD9/CD81/S100β/SOX2-positive cells will reveal the footprint pathways of adult stem/progenitor cells in the AL.

Supplementary Information The online version contains supplementary material available at https://doi.org/10.1007/s00441-021-03460-5.

Acknowledgements We are grateful to Dr. T. Kato and Y. Kato (Institute for Reproduction and Endocrinology, Meiji University) for helpful discussions. We thank the "Joint Usage/Research Center for Endocrine/Metabolism, Institute for Molecular and Cellular Regulation, Gunma University" (www.imcr.gunma-u.ac.jp/activity/activity3) for providing antibodies.

Funding This work was supported by JSPS KAKENHI Grants (nos. 19K07255 to K.H. and nos. 17K08517 to K.F.).

Declarations

Ethical approval The current study was approved by the Committee on Animal Experiments of the School of Agriculture, Meiji University, and Kyorin University based on the NIH Guidelines for the Care and Use of Laboratory Animals. This article does not contain any studies with human participants. This article does not contain any studies with human participants performed by any of the authors.

Conflict of interest The authors declare no competing interests.

References

Boucheix C, Rubinstein E (2001) Tetraspanins. Cell Mol Life Sci 58:1189–1205

Chen J, Hersmus N, Van Duppen V, Caesens P, Denef C, Vankelecom H (2005) The adult pituitary contains a cell population displaying stem/progenitor cell and early embryonic characteristics. Endocrinol 146:3985–3998

Fauquier T, Rizzoti K, Dattani M, Lovell-Badge R, Robinson IC (2008) SOX2-expressing progenitor cells generate all of the major cell types in the adult mouse pituitary gland. Proc Natl Acad Sci USA 105:2907–2912

Gremeaux L, Fu Q, Chen J, Vankelecom H (2012) Activated phenotype of the pituitary stem/progenitor cell compartment during the early-postnatal maturation phase of the gland. Stem Cells Dev 21:801–813

Hemler ME (2005) Tetraspanin functions and associated microdomains. Nat Rev Mol Cell Biol 6:801–811

Horiguchi K, Fujiwara K, Kouki T, Kikuchi M, Yashiro T (2008) Immunohistochemistry of connexin 43 throughout anterior pituitary gland in a transgenic rat with green fluorescent protein-expressing folliculo-stellate cells. Anat Sci Int 83:256–260

Horiguchi K, Fujiwara K, Yoshida S, Higuchi M, Tsukada T, Kanno N, Yashiro T, Tateno K, Osako S, Kato T, Kato Y (2014) Isolation of dendritic-cell-like S100beta-positive cells in rat anterior pituitary gland. Cell Tissue Res 357:301–308

Horiguchi K, Fujiwara K, Yoshida S, Nakakura T, Arae K, Tsukada T, Hasegawa R, Takigami S, Ohsako S, Yashiro T, Kato T, Kato Y (2018) Isolation and characterisation of CD9-positive pituitary adult stem/progenitor cells in rats. Sci Rep 8:5533

Horiguchi K, Fujiwara K, Yoshida S, Tsukada T, Hasegawa R, Takigami S, Ohsako S, Yashiro T, Kato T, Kato Y (2020a) CX3CL1/CX3CR1-signalling in the CD9/S100beta/SOX2-positive adult pituitary stem/progenitor cells modulates differentiation into endothelial cells. Histochem Cell Biol 153:385–396

Horiguchi K, Nakakura T, Yoshida S, Tsukada T, Kanno N, Hasegawa R, Takigami S, Ohsako S, Kato T, Kato Y (2016) Identification of THY1 as a novel thyrotrope marker and THY1 antibody-mediated thyrotrope isolation in the rat anterior pituitary gland. Biochem Biophys Res Commun 480:273–279

Horiguchi K, Yoshida S, Tsukada T, Nakakura T, Fujiwara K, Hasegawa R, Takigami S, Ohsako S (2020b) Expression and functions of cluster of differentiation 9 and 81 in rat mammary epithelial cells. J Reprod Dev 66:515–522

Japon MA, Rubinstein M, Low MJ (1994) In situ hybridization analysis of anterior pituitary hormone gene expression during fetal mouse development. J Histochem Cytochem 42:1117–1125

Jin Y, Takeda Y, Kondo Y, Tripathi LP, Kang S, Takeshita H, Kuhara H, Maeda Y, Higashiguchi M, Miyake K, Morimura O, Koba T, Hayama Y, Koyama S, Nakanishi K, Iwasaki T, Tetsumoto S, Tsujino K, Kuroyama M, Iwahori K, Hirata H, Takimoto T, Suzuki M, Nagatomo I, Sugimoto K, Fujii Y, Kida H, Mizuguchi K, Ito M, Kijima T, Rakugi H, Mekada E, Tachibana I, Kumanogoh A (2018) Double deletion of tetraspanins CD9 and CD81 in mice leads to a syndrome resembling accelerated aging. Sci Rep 8:5145

Matsubara M, Harigaya T, Nogami H (2001) Effects of diethylstilbestrol on the cytogenesis of prolactin cells in the pars distalis of the pituitary gland of the mouse. Cell Tissue Res 306:301–307

Ogasawara K, Nogami H, Tsuda MC, Gustafsson JA, Korach KS, Ogawa S, Harigaya T, Hisano S (2009) Hormonal regulation of prolactin cell development in the fetal pituitary gland of the mouse. Endocrinol 150:1061–1068

Oomizu S, Takeuchi S, Takahashi S (1998) Stimulatory effect of insulin-like growth factor I on proliferation of mouse pituitary cells in serum-free culture. J Endocrinol 157:53–62

Sato K, Watanabe YG (1998) Corticosteroids stimulate the differentiation of growth hormone cells but suppress that of prolactin cells in the fetal rat pituitary. Arch Histol Cytol 61:75–81

Suga H, Kadoshima T, Minaguchi M, Ohgushi M, Soen M, Nakano T, Takata N, Wataya T, Muguruma K, Miyoshi H, Yonemura S, Oiso Y, Sasai Y (2011) Self-formation of functional adenohypophysis in three-dimensional culture. Nature 480:57–62

Scully KM, Gleiberman AS, Lindzey J, Lubahn DB, Korach KS, Rosenfeld MG (1997) Role of estrogen receptor-alpha in the anterior pituitary gland. Mol Endocrinol 11:674–681

Stefaneanu L, Powell-Braxton L, Won W, Chandrashekar V, Bartke A (1999) Somatotroph and lactotroph changes in the adenohypophyses of mice with disrupted insulin-like growth factor I gene. Endocrinol 140:3881–3889

Vankelecom H, Chen J (2014) Pituitary stem cells: where do we stand? Mol Cell Endocrinol 385:2–17

Yoshida S, Kato T, Kato Y (2016a) Regulatory System for Stem/Progenitor Cell Niches in the Adult Rodent Pituitary. Int J Mol Sci 17:75

Yoshida S, Nishimura N, Ueharu H, Kanno N, Higuchi M, Horiguchi K, Kato T, Kato Y (2016b) Isolation of adult pituitary stem/progenitor cell clusters located in the parenchyma of the rat anterior lobe. Stem Cell Res 17:318–329